

Article

# Stabilization of High-Organic-Content Water Treatment Sludge by Pyrolysis

Ye-Eun Lee <sup>1,2</sup> , I-Tae Kim <sup>1</sup>  and Yeong-Seok Yoo <sup>1,\*</sup>

<sup>1</sup> Division of Environment and Plant Engineering, Korea Institute of Civil Engineering and Building Technology 283, Goyang-daero, Ilsanseo-gu Goyang-si, Gyeonggi-do 10223, Republic of Korea; yeeunlee@kict.re.kr (Y.-E.L.); itkim@kict.re.kr (I.-T.K.)

<sup>2</sup> Department of Construction Environment Engineering, University of Science and Technology, 217, Gajeong-ro, Yuseong-gu, Daejeon 34113, Republic of Korea

\* Correspondence: ysyoo@kict.re.kr; Tel.: +82-31-910-0298; Fax: +82-31-910-0288

Received: 5 November 2018; Accepted: 23 November 2018; Published: 26 November 2018



**Abstract:** Water treatment sludge from algal blooms were analyzed and compared with general water treatment sludge as the pyrolysis temperature was varied from 300 °C to 900 °C. Elemental analysis showed that the water treatment sludge in the eutrophication region has ~12% carbon content, higher than that (8.75%) of general water treatment sludge. X-ray diffraction (XRD) analysis of both types of sludge showed that amorphous silica changed to quartz and weak crystalline structures like kaolinite or montmorillonite were decomposed and changed into stronger crystalline forms like albite. Fourier transform infrared spectroscopy (FT-IR) peaks of humic/fulvic acid that indicated the affinity to combine with heavy metals disappeared above 700 °C. Toxicity characteristic leaching procedure (TCLP), conducted to determine the heavy metal leaching amount of pyrolyzed water treatment sludge, showed the lowest value of 5.7 mg/kg at 500 °C when the humic acid was not decomposed. At 500 °C, the heavy metal leaching ratio to the heavy metal content of high organic content water treatment sludge and low organic content water treatment sludge were 1.87% and 3.19%, respectively, and the water treatment sludge of higher organic content was more stable. In other words, pyrolysis of water treatment sludge with high organic content at 500 °C increases the inorganic matter crystallinity and heavy metal leaching stability.

**Keywords:** biochar; organic matter; heavy metal leaching; water treatment sludge; pyrolysis

## 1. Introduction

The increasing global population and expansion of industry have increased water usage and water pollution. As a result, more coagulants are required in water treatment facilities in order to remove pollutants, which has increased the amount of sludge generated. In South Korea, the amount of water treatment sludge had increased by more than 150 tons from 982.7 tons/day in 2011 to 1159.1 tons/day in 2016 [1,2].

Previously, water treatment sludge was treated through landfilling [3,4], but new treatment alternatives are required due to the limitations of landfill sites and the pollution of soil and underground water caused by heavy metals, as well as iron and aluminum salts in the sludge [5,6]. Three methods have attracted attention as potential alternatives: the recycling of coagulants contained in large quantities in sludge using acid treatment, the utilization of sludge in earthworks; for example, in cement mix, and the application of sludge for soil modification such as soil pH adjustment [4]. These recycling methods utilize the specific features of water treatment sludge; i.e., low organic content and high inorganic content [7].

In South Korea, population growth has increased the demand for water resources, resulting in the installation of artificial watershed structures such as dams and weirs, which affect river flow [8,9]. Due to this effect, eutrophication has worsened and caused a large amount of algal blooms. The Nakdong River, one of the major water sources in South Korea, has also encountered this problem [10–12]. The organic contents in the sludge of water treatment facilities that use the Nakdong River as a water source have increased. This is not only a problem in South Korea but a global issue related to worsening eutrophication and algal blooms [13].

An increase in sludge discharge is also associated with eutrophication and algal blooms. This is because an enhanced coagulation process that increases the input of coagulants is employed for the removal of the natural organic matter (NOM) generated by the biological activities of algae or aquatic microorganisms [14]. In other words, the discharged sludge includes not only organic matter, such as algae, but also NOM substances, which are microorganism byproducts, along with coagulants. However, research on the treatment of sludge with a high organic content, including NOM, has not been conducted. Therefore, alternatives are required for the treatment of water treatment sludge with high organic content.

Biochar is produced by applying pyrolysis to organic matter in an anoxic state and can be utilized as a soil modification substance [15]. In addition, biochar reduces the discharge of organic carbon into the air in the form of carbon dioxide by resisting microbial decomposition [16]. It is also beneficial for preventing climate change by reducing emission of greenhouse gases, such as nitrogen oxides and methane, from the soil [17].

For sewage sludge with a high organic content, many studies have already been conducted on the generation of biochar through recycling by pyrolysis. Gascó et al. [18] showed that carbon-based adsorbents can be produced by pyrolyzing unstable sewage sludge with a high organic content. He et al. [19] reported that, among the heavy metals found in sewage sludge, the stability of Cu, Zn, Pb, and Cd can be improved through pyrolysis, and Hwang et al. [20] showed that pyrolysis reduces the emission of pollutants using a leaching test of the pyrolysis byproducts of sewage sludge. Taek-keun et al. [21] investigated the characteristics of biochar obtained through the pyrolysis of various biomass waste (water treatment sludge, orange peel, and residual wood), but the research was conducted using water treatment sludge with a low organic content and focusing on the toxicity characteristics of less than the aforementioned sewage sludge.

The conversion of sewage sludge biochar by pyrolysis is good alternative to manage the waste and simultaneously environmental benefits. Agrafioti et al. [22] indicated that at low pyrolysis temperatures, the biochar produced is suitable for soil amendments, and the sewage sludge biochar produced by pyrolysis at high temperatures has soil contaminant adsorbing ability. Because sewage sludge which has higher heavy metal concentrations and a higher organic content than water treatment sludge, can be recycled as biochar for soil application through pyrolysis, we suggest that pyrolysis can also be applied to water treatment sludge with lower heavy metal concentrations as a valuable recycling method. Thus, in this study, different types of organic matter were stabilized by applying pyrolysis to the treatment of water treatment sludge with a high organic content. The structural and heavy metal leaching changes of the water treatment sludge char after pyrolysis were analyzed to determine its stability for soil applications.

## 2. Experimental

### 2.1. Raw Material

The water treatment sludge samples were collected from the Guui water treatment facility in Seoul and the Changwon water treatment facility in Changwon. The Changwon water treatment facility used a water with a large amount of algal blooms as a water resource. The wet water treatment sludge samples were transformed into powder by drying at 105 °C for 48 h, grinding, and sieving through a 1.18-mm sieve.

## 2.2. Experimental Methods

The water treatment sludge samples were pyrolyzed at 300, 500, 700, and 900 °C in a furnace; oxidation reactions was prevented by introducing nitrogen gas at a flow rate of 10 L/min. The temperature was increased to 300, 500, 700, and 900 °C at 20 °C /min, and the pyrolysis was conducted at the target temperature for 1 h. Samples (70 g) were then placed into containers with dimensions of 50 × 200 × 45 mm and placed in the furnace at the target temperature. And the experimental pyrolysis system is set like Figure 1. After the samples had completed the pyrolysis they were cooled to room temperature and weighed. Gas produced during the pyrolysis process was released through an exhaust fan after combustion.

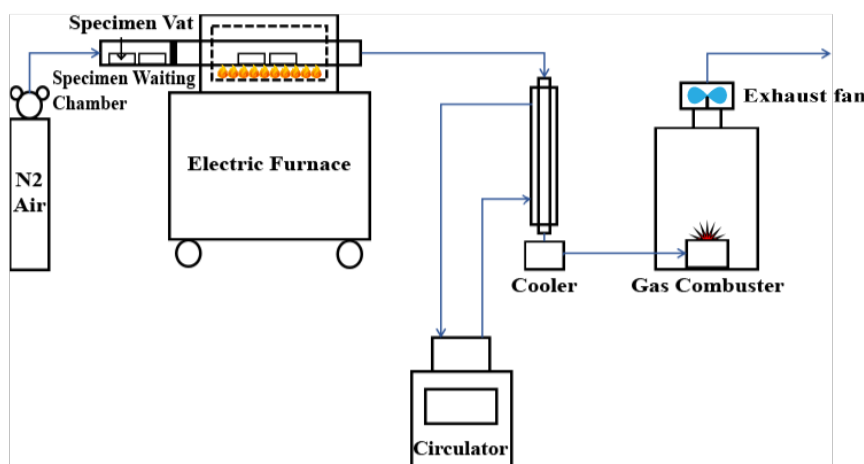


Figure 1. Configuration of the pyrolysis experiment setup.

## 2.3. Analytical Methods

### 2.3.1. Characterization

A CHNS analyzer (2400 Series II CHNS/O, Perkin Elmer, Boston, MA, USA) was used to obtain the elemental compositions of the water treatment sludge samples and the sludge char after pyrolysis. X-ray fluorescence spectrometry (XRF) analysis was conducted to analyze the chemical composition of each sample using Axios equipment (Malvern PANalytical Co., Ltd, Royston, UK). For the proximate analysis of each dried water treatment sludge sample, moisture, volatile matter, ash, and fixed carbon contents were analyzed in accordance with KS E 3804 (natural graphite proximate analysis and test method). The moisture content was obtained by placing each sample into a porcelain crucible, measuring its weight, measuring its weight again after heating at 100–105 °C for 2 h, and calculating the difference in weight. For the volatile matter content, a dried sample was placed into a porcelain crucible and weighed. After the lid was closed, it was heated at  $950 \pm 20$  °C for 7 min and weighed again to calculate the difference in weight. The ash content was obtained by calculating the difference between the weight measured when a completely dried sample was placed into the porcelain crucible and the weight measured when the sample was heated at 850 °C for 3 h. The fixed carbon content was calculated by assuming 100% for a completely dried sample and subtracting the volatile matter and ash contents (%).

### 2.3.2. Structural Analysis

X-ray diffraction analysis was conducted to examine the structural changes in the char. A DMAX 2500 system (Rigaku, Tokyo, Japan) was used for the analysis, and the X-ray generator had specifications of 18 kW 60 kV/300 mA. The  $2\theta$  range of the recorded sample was 10–90°. For Fourier transform infrared spectroscopy (FT-IR), a VERTEX 80V spectrometer (Bruker Optics, Billerica, MA, USA) was used, and the KBr pellet method was applied, whereby a sample (1 mg) is mixed with KBr

powder and a thin film produced by pressurizing the mixture. Changes in the organic structure inside the sample during pyrolysis were examined using infrared rays with wavelengths between 400 nm and 4000 nm.

### 2.3.3. Heavy Metal Leaching Analysis

Experiments and analysis were conducted to examine the heavy metal content in water treatment sludge, as well as the change in the heavy metal leaching amount after pyrolysis. The heavy metal content was analyzed using an Agilent 5100 ICP-OES instrument (Agilent Technologies, Santa Clara, CA, USA) after performing pretreatment in accordance with the soil pollution process test method of South Korea. The heavy metal leaching amount was also analyzed using the Agilent 5100 ICP-OES after performing pretreatment in accordance with the Toxicity Characteristic Leaching Procedure (TCLP; US EPA Method 1311): two acetic acid fluids of pH 4.93 and 2.88 were prepared. The 10g of samples were added to the higher pH solution (when the extraction of sample's pH less than 5) and agitated for the extraction. The lower pH solution was used for extraction when the sample's pH was above 5.

## 3. Results and Discussion

### 3.1. Water Treatment Sludge and Water Treatment Sludge Char Composition Analysis

For both the water treatment sludge from the facility with a large amount of algal blooms due to eutrophication (CW sludge) and that from the water treatment facility without algal blooms (GU sludge), the elemental and chemical compositions were analyzed. Table 1 shows the results of the proximate analysis of the dried water treatment sludge samples, and Table 2 shows the elemental composition analysis results for the dried and pyrolyzed water treatment sludge samples according to temperature. As shown in Table 1, CW sludge exhibited higher volatile matter content and lower ash content than GU sludge. The fixed carbon content of CW sludge was also higher than that of GU sludge. This confirms that the water treatment sludge from the area with a large amount of algal blooms has a high organic content. Table 3 shows the yield values of each water treatment sludge after pyrolysis. The water treatment sludge with higher ash content showed higher yield value. The higher ash content and lower organic content inhibit volatilization of the organic content and increase the yield value.

**Table 1.** Results of dried sludge proximate analysis for each water treatment facility.

Sample	Moisture Content	Volatile Matter Content	Ash Content	Fixed Carbon Content
CW	8.17 ± 0.47	30.90 ± 0.10	63.5 ± 0.47	5.63 ± 0.40
GU	4.76 ± 0.51	25.20 ± 0.55	71.1 ± 0.43	3.69 ± 0.13

**Table 2.** Elemental composition analysis results for the dried and pyrolyzed byproducts of each water treatment facility.

Sample	C	H	N	O	H/C	C/N
CW Dried	11.96 ± 0.17	2.77 ± 0.06	1.58 ± 0.03	10.98 ± 0.49	0.23	7.59
CW 300	11.89 ± 0.75	1.93 ± 0.35	1.66 ± 0.02	10.33 ± 3.38	0.16	7.16
CW 500	8.46 ± 0.32	1.26 ± 0.02	0.97 ± 0.02	2.79 ± 0.50	0.15	8.76
CW 700	8.32 ± 0.36	0.71 ± 0.00	0.65 ± 0.02	4.77 ± 0.94	0.09	12.79
CW 900	5.82 ± 1.03	0.20 ± 0.07	0.24 ± 0.04	4.40 ± 2.04	0.03	24.52
GU Dried	8.75 ± 0.11	2.25 ± 0.20	1.17 ± 0.08	9.15 ± 0.26	0.26	7.50
GU 300	8.82 ± 0.69	1.77 ± 0.01	1.28 ± 0.06	8.09 ± 0.01	0.20	6.89
GU 500	6.07 ± 0.07	1.06 ± 0.03	0.65 ± 0.01	4.32 ± 0.47	0.18	9.29
GU 700	5.31 ± 0.78	0.60 ± 0.02	0.44 ± 0.01	3.64 ± 0.12	0.11	12.21
GU 900	6.77 ± 0.04	0.18 ± 0.08	0.22 ± 0.03	2.16 ± 0.15	0.03	30.77

**Table 3.** Yields of each water treatment sludge char residue.

Sample	Yield (%)				Organic Matter Yield (%)			
	300 °C	500 °C	700 °C	900 °C	300 °C	500 °C	700 °C	900 °C
CW	82.41 ± 1.65	71.45 ± 0.96	66.08 ± 0.58	63.80 ± 0.25	51.76	21.75	7.05	0.83
GU	89.62 ± 1.64	79.89 ± 0.67	74.23 ± 0.61	71.74 ± 0.03	64.09	30.42	10.84	2.21

Biochar yield means organic carbon residue. But this research contains much of inorganic matter. So, considering organic content (CW:30.9%, GU:25.2%), inorganic content, and fixed carbon (Ash content\_CW:63.5%, GU:71.1%) and recalculated using the following formula:

$$\frac{\text{Yield value (\%)} - \text{Ash content (CW : 63.5\%, GU : 71.1\%)}}{\text{organic content (CW : 30.9\%, GU : 25.2\%)} + \text{fixed carbon (CW : 5.63\%, GU : 3.69\%)}} = \text{Organic matter yield (\%)}$$

For the CW sludge with a high organic content, the carbon, nitrogen, and oxygen contents decreased at higher pyrolysis temperatures. For the GU sludge with lower organic content, the carbon, nitrogen, and oxygen contents also decreased as the pyrolysis temperature increased, although the carbon content increased only at 900 °C. The H/C and O/C values are criteria for determining the stability of biochar [23,24]. As these values decrease, the aromaticity and maturation of the organic matter increase. However, the sample stability could not be determined using the O/C value because a large amount of oxygen was combined with the inorganic matter. Nonetheless, the increase in stability was confirmed by the fact that the H/C value decreased as the pyrolysis temperature increased for both sludges. The C/N ratio can also be used. A high C/N ratio is an indicator of mineralization and nitrogen release in soils [24]. Biochar used for soil should have a C/N ratio equal to or higher than 8 [25]. Satisfactory values were obtained at 500 °C or higher pyrolysis temperatures, indicating an increased degree of N immobilization and thus stability as the pyrolysis temperature increased, as with the H/C value. Table 4 shows the XRF analysis results of the water treatment sludge samples. CW sludge and GU sludge did not exhibit a significant difference in their basic composition and contents, but CW sludge exhibited higher phosphorus and sulfur contents than GU sludge.

**Table 4.** X-ray fluorescence spectrometry (XRF) analysis results for the dried water treatment sludge and the water treatment sludge by pyrolysis temperature (°C).

(%)	CW Dried	300	500	700	900
Si	25.13	25.04	25.19	25.24	25.32
Al	16.58	17.51	18.01	18.23	18.06
Fe	3.90	3.64	3.46	3.33	3.56
K	1.15	1.09	1.07	1.07	1.17
S	1.02	0.75	0.41	0.18	0.19
Ca	0.90	0.79	0.74	0.74	0.83
P	0.58	0.56	0.54	0.61	0.46
Cl	0.39	0.34	0.31	0.25	0.09
Mg	0.34	0.36	0.36	0.45	0.49
Ti	0.32	0.30	0.28	0.28	0.32
Na	0.19	0.22	0.22	0.28	0.31
Si	25.26	25.05	25.16	25.18	25.45
Al	17.05	17.73	17.93	18.30	18.07
Fe	4.25	3.76	3.77	3.70	3.63
K	1.36	1.28	1.27	1.25	1.17
Ca	0.95	0.84	0.87	0.86	0.80
Mg	0.46	0.53	0.53	0.51	0.45
S	0.50	0.46	0.27	0.11	0.14
Cl	0.42	0.43	0.41	0.26	0.09
P	0.36	0.39	0.36	0.34	0.42
Ti	0.40	0.36	0.36	0.36	0.33
Na	0.22	0.28	0.26	0.26	0.28

This is likely because the water source of the area with algal blooms also has a high phosphorus content. Chlorine and sulfur contents decreased as the pyrolysis temperature increased (Table 4). This is because chlorine and sulfur were volatilized while other substances were not easily volatilized during the pyrolysis process because they existed in crystalline forms. The emitted trace pollutants in the form of liquids or gases during the pyrolysis need to be further investigated.

### 3.2. FT-IR Analysis

When the dried samples of the CW sludge and GU sludge were compared, there was no difference in peak positions. Both samples exhibited similar peaks, and changes occurred according to the pyrolysis temperature. Figure 2 shows the FT-IR results of the two treated water samples according to their drying and pyrolysis temperature. Table 2 summarizes the major peaks, of which three types were observed, appearing peaks, disappearing peaks, and moving peaks, as the pyrolysis temperature increased. First, the appearing peaks are those at 560, 720, 770, 790, and 1160  $\text{cm}^{-1}$ . The peaks at 770, 790, 1080, and 1160  $\text{cm}^{-1}$  appeared due to the stretching vibration of the Si-O band of quartz [26]. Previously blurred peaks became clearer as the pyrolysis temperature increased. This is because the residual quartz component became clearer as other substances were volatilized. The XRD results in Figure 3 confirm that the quartz component remained as it was despite the high pyrolysis temperatures, but other crystals such as montmorillonite were decomposed, thereby reducing and removing the peaks. Second, the disappearing peaks are those at 530–540, 910, 1010, 1040, 1240, 1380–1460, 1560, 2850, 2920, 2960, 3620, and 3700  $\text{cm}^{-1}$ .

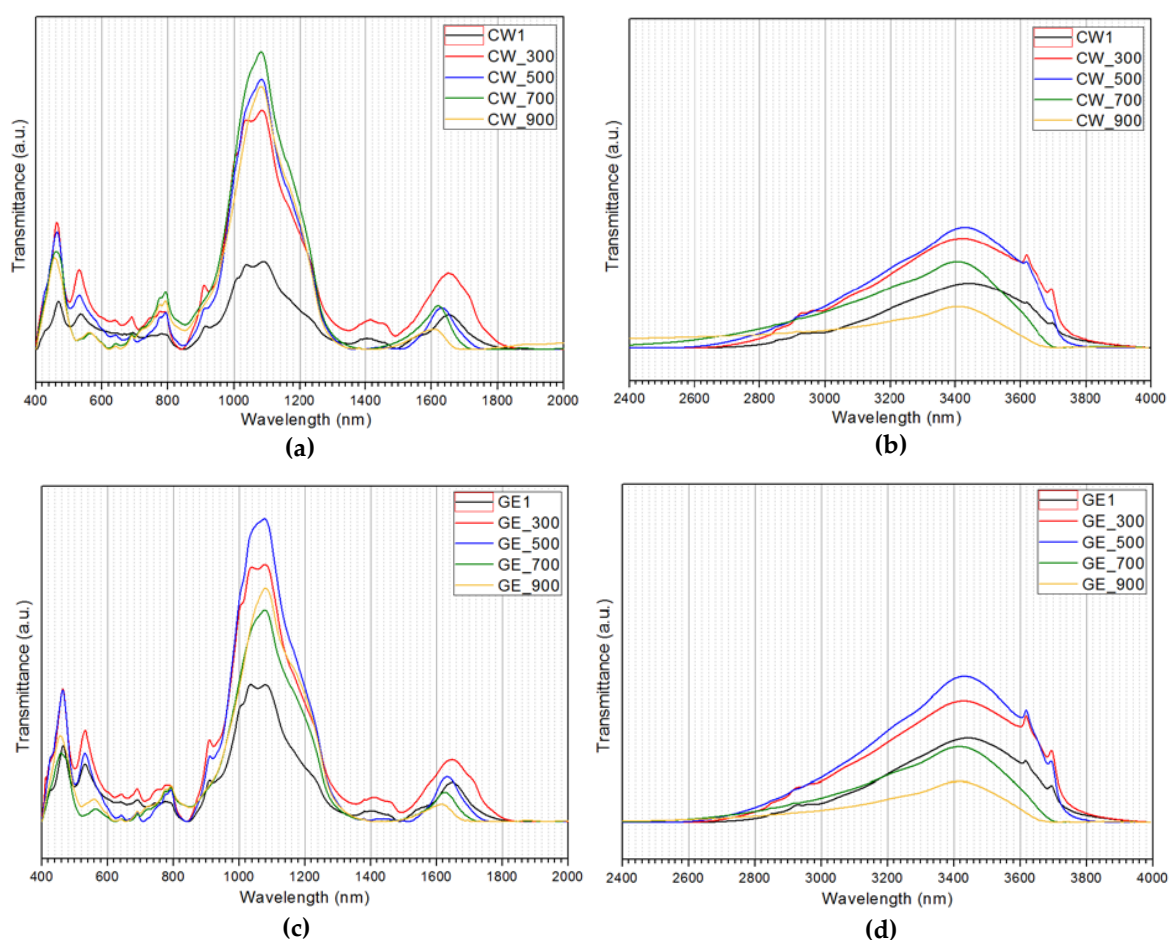


**Figure 2.** FT-IR results for the two types of sludge in different wavelength ranges: (a) CW 400–2000  $\text{cm}^{-1}$ , (b) CW 2000–4000  $\text{cm}^{-1}$ , (c) GU 400–2000  $\text{cm}^{-1}$ , and (d) GU 2000–4000  $\text{cm}^{-1}$ .

Table 5 shows that the bond between nitrogen and alcoholic and phenolic OH, aliphatic and aromatic C-H, or carbon, or the bond between the halogen substances is gone. The peaks at 470, 530, 910, 1030, 3620, and 3440  $\text{cm}^{-1}$  represent illite-montmorillonite [26–28]. According to Zhang et al. [29] humic acids showed FT-IR peaks at 470, 540, 910, 1040, 1100, 1385, 1600, 2850, 2925, 3420, 3620, and 3690  $\text{cm}^{-1}$ , and fulvic acid showed peaks at 570, 630, 1035, 1235, 1560, 2925, and 3420  $\text{cm}^{-1}$ . In a study by Wu et al. [30], HA/Ca-Mont, in which humic acids and montmorillonite are combined, exhibited peaks at 520, 795, 840, 915, 1035, 1088, 1642, 3445, and 3620  $\text{cm}^{-1}$ . When heavy metals, such as Cu and Cd, were bonded to HA/Ca-Mont, peak shifting was observed near 1640, 1090, and 3440  $\text{cm}^{-1}$ .

**Table 5.** Assignments of each FT-IR peak band.

Band Position ( $\text{cm}^{-1}$ )	Component
450–470	Aromatic rings C-C stretching 470: Si-O-Si
790, 875, 1190	$\text{CO}_3^{2-}$
910	OH bending bounded 2 $\text{Al}^{3+}$
1010	C-H deformation substituted aromatics
1030–1040	Si-O, C-N stretching, C-O stretching
1080–1090	C-O-C ether
1160	C-O-C ester groups in cellulose
1380–1460	1416 (aromatic ring -), 1460-Stretching of C=O in cyclic amides 1375 phenolic O-H bending, 1440 aromatic C=C stretching 1645(C=O in cyclic amides) 1630 (Aromatic C-C ring stretching, 1643 (H-O-H bending)-
1600–1660	1550–1680 quinones 1600 aromatic C-C or quinones's C=O
2850, 2920, 2960	2850, 2920 (aliphatic CH <sub>2</sub> stretching) 2960 (aliphatic ethers), alkyl/aliphatic C-H stretching
3400–3440	Alcoholic and phenolic OH stretching

In other words, as the pyrolysis temperature increased, the decomposition and change of the humic acids, fulvic acids, and montmorillonite occurred in the sludge. In particular, the fact that the peaks near 3620 and 3700  $\text{cm}^{-1}$  observed for the humic acids (HA) disappeared from 700 °C indicates that decomposition of HA occurred at high temperatures. The peak movement observed near 1080, 1640, and 3440 confirms that there were changes in the binding with heavy metals.

The peaks at 2850, 2920, and 2960  $\text{cm}^{-1}$  were caused by aliphatic C-H stretching. The disappearance of these peaks means that aliphatic carbon substances were decomposed. The aromatic carbon peak at 1380–1460  $\text{cm}^{-1}$  also disappeared at pyrolysis temperatures higher than 300 °C. These indicate that organic substances including carbon were decomposed and stabilized as the pyrolysis temperature increased. Guizani et al. [31] also showed as the pyrolysis temperature increases, the amorphous carbon compounds is vanished and aromatic carbon compound content is increased.

Finally, peak movement was confirmed at 470, 1090, 1660, and 3440  $\text{cm}^{-1}$ . The peaks that appeared at 470, 1090, 1660, and 3440  $\text{cm}^{-1}$  in the dried state gradually moved to the left as the pyrolysis temperature increased; the peaks appeared at 455–460, 1080, 1600, and 3400  $\text{cm}^{-1}$  when pyrolysis was performed at 900 °C. The peak movement at 470 was associated with deformation of montmorillonite or decomposition of humic acids, as mentioned earlier. The peak movement from 1090 to 1080  $\text{cm}^{-1}$  was caused by a change in the Si-O-Si structure. Danková et al. [28] and Tantawy et al. [32] showed that the content of amorphous silica increased because the peak at 1050  $\text{cm}^{-1}$  changed to a peak of Si-O free vibration at 1095  $\text{cm}^{-1}$  when nitric acid and heat were applied. Therefore, the fact that the peak moved from 1090 to 1080  $\text{cm}^{-1}$  as the pyrolysis temperature increased can be construed as a change of amorphous silica to crystal quartz, indicating that the stability of the inorganic matter was increased. The peak movement at 1660 and 3440  $\text{cm}^{-1}$  indicates that the aromatic carbon or COOH

and OH components [33] were decomposed and volatilized as the pyrolysis temperature increased and the amount of binding that induced the corresponding vibration was reduced.

### 3.3. XRD Analysis

Figure 3 shows the XRD results of the dried sludge and pyrolyzed sludge in CW and GU water treatment facilities. First, as for the structural changes of the dried sludge and pyrolyzed sludge with pyrolysis temperature, GU sludge with a low organic content showed peaks at 12.5, 19.9, 21, 22, 23.5, 24.3, 26.6, 28, 35, 35.3, 36.5, 38.6, 39.5, 40.3, 42.5, 50.2, 60, and 68.2, and some peaks disappeared or appeared depending on the pyrolysis temperature. CW sludge exhibited peaks at 12.5, 19.9, 20.8, 22, 23.5, 24.3, 26.6, 28, 35, 36.5, 39.5, 40.3, 41.6, 42.5, 45.7, 50.2, 60, and 68.2, which were similar to the peaks of GU sludge. The peaks at 20.8, 21, 26.6, 36.5, 39.5, 40.3, 42.5, 45.7, 50.2, 60, and 68.2, which were observed from both samples and did not exhibit significant peak changes, represent quartz [26,34–37]. This indicates that there was no change in quartz crystals with pyrolysis temperature.

The most obvious difference between the two dried sludge samples was the peak at 38.6°. The kaolinite ( $\text{Al}_2\text{Si}_2\text{O}_5(\text{OH})_4$ ), which includes a peak at  $38.6^\circ$ , exhibits peaks at 12.5, 19.9, 22, 35.3, and  $38.6^\circ$ . The kaolinite peak that appeared only in GU sludge gradually decreased or disappeared as the pyrolysis temperature increased.

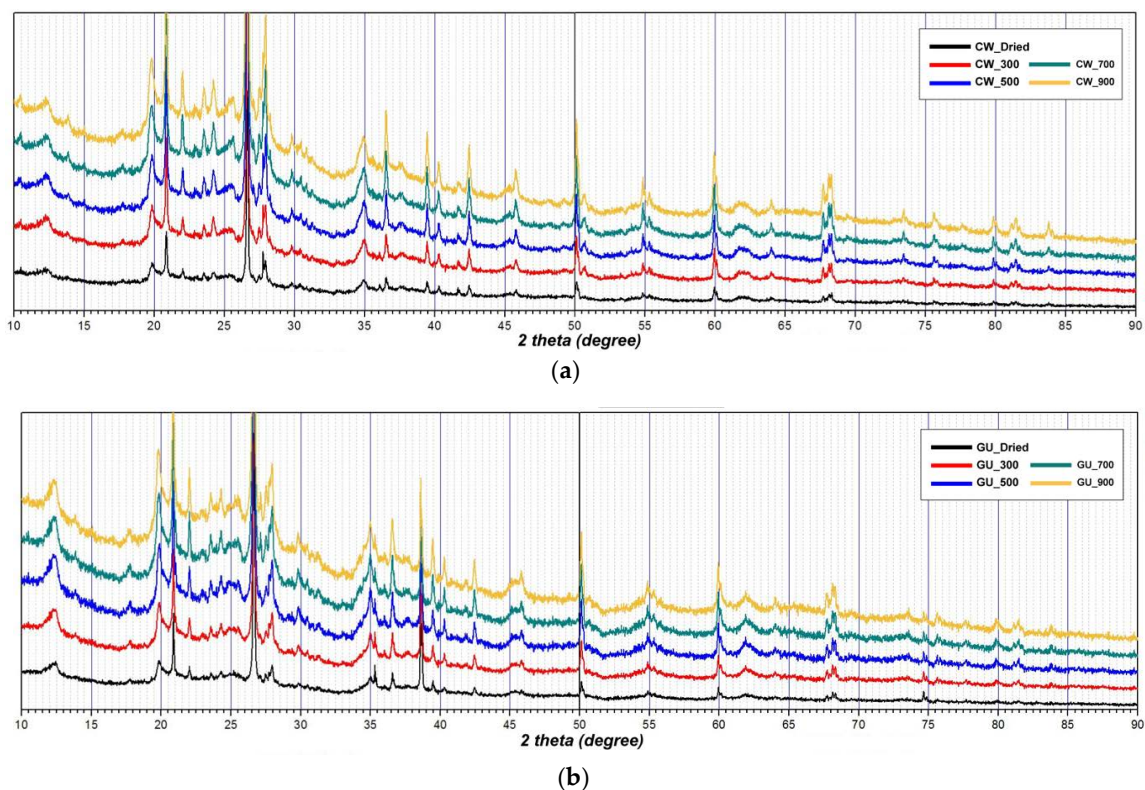


**Figure 3.** X-ray diffraction (XRD) results of water treatment sludge and pyrolyzed char for (a) CW and (b) GU.

In other words, kaolinite crystals collapsed as the pyrolysis temperature increased. The peaks at 19.9 and  $35^\circ$  are the peaks of montmorillonite. The peak at  $19.9^\circ$ , which appeared for both samples, moved to the left when the pyrolysis temperature increased to 700 and  $900^\circ\text{C}$ , and the peak at  $35^\circ$  disappeared at  $700^\circ\text{C}$  and  $900^\circ\text{C}$ . This indicates that the montmorillonite crystals included in the water treatment sludge were decomposed at high pyrolysis temperatures. The peaks at 22, 23.5, 24.3, 28, and  $41.6^\circ$  represent albite. These peaks lasted up to  $700^\circ\text{C}$  and became blurred at  $900^\circ\text{C}$ . The peak that appeared at  $28^\circ$  was weakened from  $700^\circ\text{C}$ , and the peak at  $27.5^\circ$  appeared at  $700^\circ\text{C}$  and  $900^\circ\text{C}$ .

These indicate that albite also changed at high temperatures. Crystals with relatively low strengths, such as kaolinite and montmorillonite, were decomposed as the temperature increased, while crystals with high strengths, such as albite, lasted longer. In addition, amorphous silica was also converted into quartz with high strength, indicating that the stability of inorganic matter increased as the pyrolysis temperature increased.

### 3.4. Heavy Metal Leaching Analysis

Experiments and analysis were conducted to examine the heavy metal content in the water treatment sludge, as well as the change in the heavy metal leaching amount after pyrolysis. After the pyrolysis, the heavy metal content was quantitatively analyzed and TCLP analysis was conducted at each temperature to determine if heavy metal was released due to rainwater resulting in a new environmental problem when the produced sludge char was reused as a soil amendment or building and construction aids. A TCLP analysis reveals the amount of heavy metal that can be released by acid solution. Table 6 shows the heavy metal contents of CW sludge and GU sludge with pyrolysis temperature and the heavy metal contents of the dried sludge.

For the CW sludge with a high organic content, the overall heavy metal content was relatively low. For CW sludge, arsenic and cadmium were concentrated near 500–700 °C as the pyrolysis temperature increased, but their contents tended to decrease afterwards due to volatilization. On the other hand, lead, copper, nickel, and zinc were continuously concentrated up to 900 °C, with copper exhibiting the largest variation. For the GU sludge, cadmium showed a similar tendency to CW sludge, but arsenic content did not exhibit significant changes. Lead and zinc also exhibited a reduction in content, whereas they were continuously concentrated up to 900 °C in CW sludge.

The vaporization temperature of zinc is approximately 907 °C; thus, the amount of zinc decreased because zinc was volatilized in small quantities when the GU sludge was pyrolyzed. For CW sludge, on the other hand, although zinc was volatilized in small quantities, the volatilization of organic matter increased significantly, thereby increasing the concentration of zinc and making it appear to have increased without being volatilized.

For GU sludge, most heavy metals, such as copper, nickel, zinc, arsenic, and lead, did not show constant trends and their increase or decrease was not clear. This appears to be because GU sludge had low organic content; thus, the change in content due to the change in volatilization caused by the pyrolysis temperature was not significant. For CW sludge, the concentration of heavy metals was relatively obvious because a large amount of organic matter was volatilized due to the high organic content as the pyrolysis temperature increased.

Figure 4 shows the heavy metal contents of CW sludge and GU sludge, the leaching amounts in accordance with TCLP, and the leaching amounts compared to the heavy metal contents according to the pyrolysis temperature. The line graph of Figure 4 that represents the leaching amount compared to the content shows that GU and CW sludges exhibited similar tendencies for all heavy metals except lead.

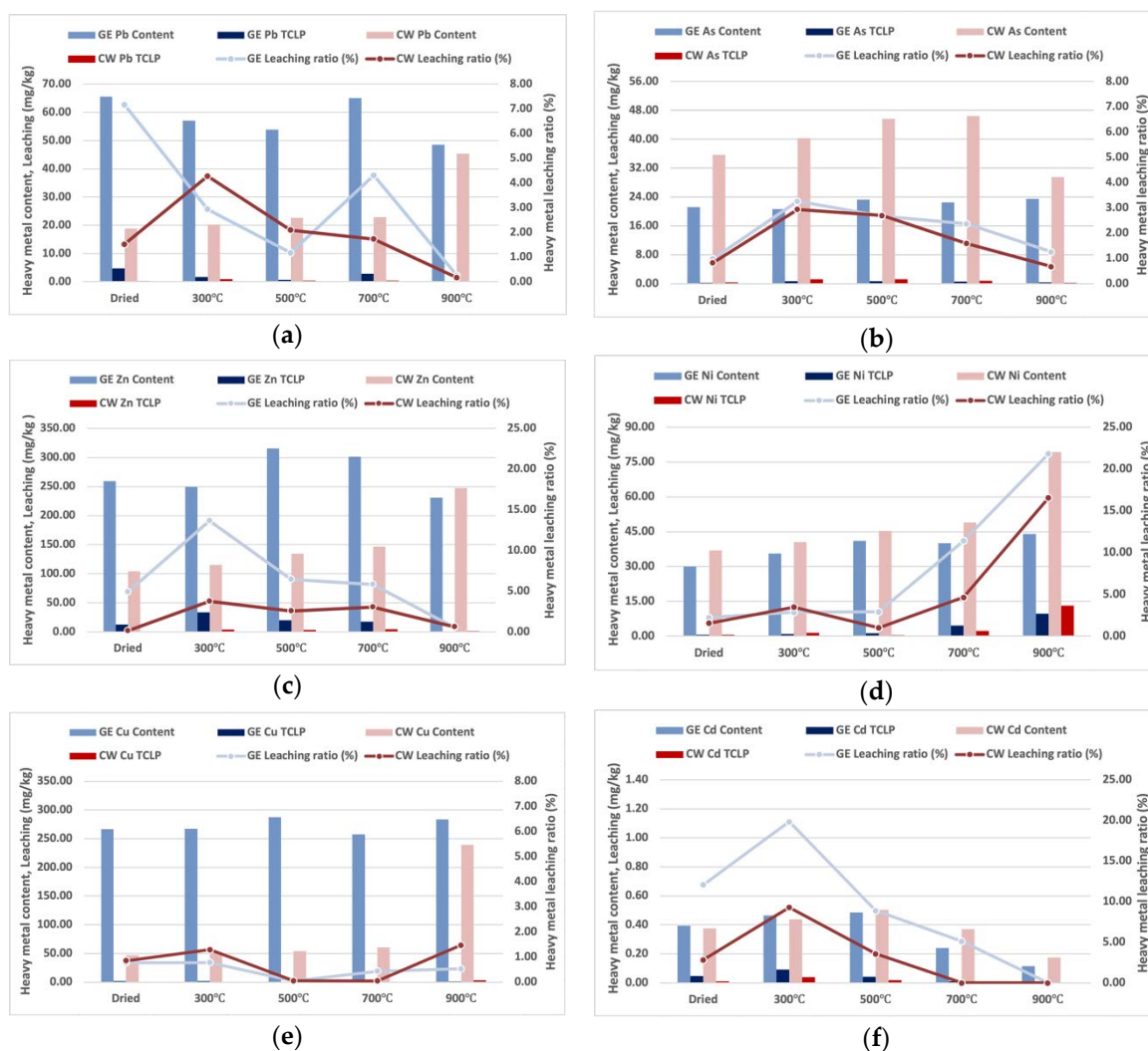


**Figure 4.** Amounts of heavy metals in biochar according to the pyrolysis temperature: (a) Pb; (b) As; (c) Zn; (d) Ni; (e) Cu; (f) Cd.

The biochar obtained by pyrolyzing CW sludge typically had a smaller leaching amount to heavy metal amount ratio than the biochar obtained by pyrolyzing GU sludge, except for Cu. The heavy metal leaching ratio to each heavy metal content shows two types of behaviors. First, the leaching ratio tends to decrease as the pyrolysis temperature increases from 300 to 900 °C, second, the releasing ratio is gradually increases at temperatures above 500 °C. The former trend is shown by Pb, As, Zn, and Cd, and the latter by Cu and Ni. The tendency of increasing leaching ratio at temperatures above 500 °C can be interpreted in terms of the decomposition of humic acids. The humic acids that have affinity to combine with heavy metals were decomposed at a temperature above 500 °C, and Wu et al. [30], showed that Cu has high affinity to humic acids. Second, the tendency of constantly decreasing leaching ratio can be understood in several ways. First, as for As and Cd, as the pyrolysis temperature increases, the amount of volatilization is increased, resulting in a decrease in elution. In the case of Pb and Zn, it can be interpreted that the surface area of char increases as the pyrolysis temperature increases [22,24], resulting in decreased elution due to the adsorption capacity. Similar to this result, Y.D. et al.'s [19] study on sewage sludge pyrolysis also showed that Pb and Zn leaching amount decreases as the pyrolysis temperature increases.

**Table 6.** Heavy metal contents at different pyrolysis temperatures.

(mg/kg)	Arsenic	Cadmium	Lead	Copper	Nickel	Zinc
CW	35.63 ± 0.26	0.38 ± 0.02	18.84 ± 0.39	46.61 ± 0.17	36.96 ± 0.25	104.06 ± 0.88
CW_300 °C	40.33 ± 2.24	0.44 ± 0.00	20.28 ± 0.22	50.62 ± 0.29	40.64 ± 0.73	115.34 ± 4.14
CW_500 °C	45.67 ± 0.30	0.51 ± 0.02	22.61 ± 0.25	54.30 ± 0.84	45.38 ± 0.81	134.52 ± 0.88
CW_700 °C	46.46 ± 3.27	0.37 ± 0.04	22.95 ± 0.47	60.88 ± 1.57	49.03 ± 0.62	147.16 ± 0.50
CW_900 °C	29.58 ± 3.07	0.18 ± 0.05	45.41 ± 4.68	239.51 ± 35.47	79.32 ± 27.73	247.59 ± 41.89
GE	21.16 ± 2.07	0.40 ± 0.06	65.59 ± 14.37	266.58 ± 78.97	29.94 ± 0.07	259.19 ± 34.43
GU_300 °C	20.60 ± 0.88	0.47 ± 0.01	57.09 ± 2.89	267.53 ± 38.07	35.58 ± 1.48	249.74 ± 1.36
GU_500 °C	23.32 ± 0.31	0.49 ± 0.03	53.80 ± 2.31	287.54 ± 9.41	41.09 ± 3.38	315.76 ± 3.64
GU_700 °C	22.49 ± 0.50	0.24 ± 0.03	65.05 ± 1.47	257.81 ± 12.80	40.07 ± 2.97	301.53 ± 13.14
GU_900 °C	23.44 ± 2.46	0.12 ± 0.02	48.50 ± 10.75	283.80 ± 20.11	44.10 ± 1.33	230.85 ± 11.25

Figure 5 shows the heavy metal contents, total leaching amount, and total leaching amount compared to the total content for different pyrolysis temperatures. CW sludge biochar generally showed a lower total heavy metal content than the GE sludge biochar. However, at 900 °C, with high organic matter volatilization, its total amount significantly increased because heavy metals became concentrated. The leaching amount to content ratio was generally smaller for CW sludge biochar with high organic content, but the leaching amount to content ratio for CW sludge biochar was larger at 900 °C, at which temperature the carbon content was lower than in the GE sludge due to high organic matter volatilization.

The results at 900 °C indicate that the heavy metals leaching amount is associated with the organic content. Among various NOM substances included in sludge, humic acids and fulvic acids are highly likely to form organometallic complexes by forming strong bonds with heavy metals [14,38,39]. When some of the organic matter bonded with heavy metals is decomposed and exposed to acids through the TCLP leaching test during pyrolysis at 300 °C, the organic matter and heavy metals are leached together, increasing the leaching amount. However, when sufficient carbonization occurs at 500 °C or higher, heavy metals are captured along with stabilization of the carbon.



**Figure 5.** Total heavy metal amounts in biochar according to pyrolysis temperature. (T: Total content, L: Leaching amount, LR: Leaching amount/Total content).

A comparison between the carbon content at 500 °C or higher and the leaching amount compared to the heavy metal content of Figure 5 confirms that the organic content that captures heavy metals decreases as the pyrolysis temperature increases in CW sludge. This then increases the leaching amount. In the case of GU sludge, the leaching amount is also inversely correlated to the increase or decrease in carbon content, and the leaching amount is lower at 900 °C, at which temperature the carbon content is

higher than in CW sludge. In other words, it was confirmed that the leaching amount of heavy metals is closely related to the stability of the organic matter. Until now, water treatment sludge has been recycled and reused as a coagulant in sewage treatment, building and construction aids, or soil pH buffer. However, highly organic water treatment sludge cannot be recycled as mentioned because of its organic content, and heavy metal leaching could also be a considerable problem. The results of this study demonstrate that there is a good possibility of recycling high organic content water treatment sludge. This is because high organic content sludge can be stabilized through thermal decomposition that reduces the heavy metal leaching rate and induces stronger crystallization of minerals, which is beneficial for their use as light-weight aggregates and also ensures stability for application as soil improvement agents.

#### 4. Conclusions

In this study, high organic content water treatment sludge due to the eutrophication of water resource was pyrolyzed at 300 to 900 °C for stabilization of organic content, and the structure and heavy metal leaching change were analyzed as the pyrolysis temperature variation to confirm the soil adjustment. The carbon contents and phosphorus contents in the sludge of water treatment facilities that use the eutrophication occurred water source are 3.21% and 0.22% higher, respectively, than the sludge of a general water treatment facility. The carbon matter contained in the sludge was decomposed into a stable form as the pyrolysis temperature increases. The FT-IR and XRD analysis results have shown that the mineral material also gradually changed into a strong crystalline form. The FT-IR peaks of the humic acids that prefer to bind with heavy metals disappeared at temperatures above 700 °C, resulting in a gradual increase in heavy metal leaching ratio. Accordingly, pyrolysis of sludge with a high organic content at 500 °C reduces the amount of heavy metal release and increases organic and inorganic content stability, which could be a good alternative for sludge treatment.

**Author Contributions:** Conceptualization, Y.-E.L. and Y.-S.Y.; Validation, Y.-E.L., Y.-S.Y.; Formal Analysis, Y.-E.L.; Investigation, Y.-E.L.; Resources, Y.-E.L.; Writing-Original Draft Preparation, Y.-E.L.; Writing-Review & Editing, Y.-E.L., Y.-S.Y., and I.-T.K.; Supervision, Y.-S.Y.; Project Administration, I.-T.K.

**Funding:** This work was supported by the Major Project of the Korea Institute of Civil Engineering and Building Technology (KICT) (grant number 2018-0063).

**Conflicts of Interest:** The authors declare no conflict of interest.

#### References

1. Ministry of Environment (MOE). *National Waste Generation and Processing Statistics*; Ministry of Environment: Sejong City, Korea, 2016.
2. Ministry of Environment (MOE). *National Waste Generation and Processing Statistics*; Ministry of Environment: Sejong City, Korea, 2011.
3. Yang, Y.; Tomlinson, D.; Kennedy, S.; Zhao, Y. Dewatered alum sludge: A potential adsorbent for phosphorus removal. *Water Sci. Technol.* **2006**, *54*, 207–213. [[CrossRef](#)] [[PubMed](#)]
4. Ahmad, T.; Ahmad, K.; Alam, M. Characterization of water treatment plant's sludge and its safe disposal options. *Procedia Environ. Sci.* **2016**, *35*, 950–955. [[CrossRef](#)]
5. Sales, A.; Francis Rodrigues de Souza. Concretes and mortars recycled with water treatment sludge and construction and demolition rubble. *Construct. Build. Mater.* **2009**, *23*, 2362–2370. [[CrossRef](#)]
6. Chen, H.; Ma, X.; Dai, H. Reuse of water purification sludge as raw material in cement production. *Cem. Concr. Comp.* **2010**, *32*, 436–439. [[CrossRef](#)]
7. Babatunde, A.O.; Zhao, Y.Q. Constructive approaches toward water treatment works sludge management: An international review of beneficial reuses. *Crit. Rev. Environ. Sci. Technol.* **2007**, *37*, 129–164. [[CrossRef](#)]
8. Magilligan, F.J.; Nislow, K.H. Changes in hydrologic regime by dams. *Geomorphology* **2005**, *71*, 61–78. [[CrossRef](#)]
9. Kim, D.K.; Jeong, K.S.; Whigham, P.A.; Joo, G.J. Winter diatom blooms in a regulated river in South Korea: Explanations based on evolutionary computation. *Freshw. Biol.* **2007**, *52*, 2021–2041. [[CrossRef](#)]

10. Lee, S.-H.; Kim, B.-R.; Lee, H.-W. A study on water quality after construction of the weirs in the middle area in Nakdong River. *J. Korean Soc. Environ. Eng.* **2014**, *36*, 258–264. [[CrossRef](#)]
11. Jung, K.Y.; Lee, K.-L.; Im, T.H.; Lee, I.J.; Kim, S.; Han, K.-Y.; Jung, M.A. Evaluation of water quality for the Nakdong River watershed using multivariate analysis. *Environ. Technol. Innov.* **2016**, *5*, 67–82. [[CrossRef](#)]
12. Andinet, T.; Kim, I.; Kim, J. Mini-review on river eutrophication and bottom improvement techniques, with special emphasis on the Nakdong River. *J. Environ. Sci.* **2015**, *30*, 113–121.
13. Binzer, A.; Guill, C.; Rall, B.C.; Brose, U. Interactive effects of warming, eutrophication and size structure: Impacts on biodiversity and food-web structure. *Glob. Chang. Biol.* **2016**, *22*, 220–227. [[CrossRef](#)] [[PubMed](#)]
14. Sillanpää, M.; Ncibi, M.C.; Matilainen, A.; Vepsäläinen, M. Removal of natural organic matter in drinking water treatment by coagulation: A comprehensive review. *Chemosphere* **2018**, *190*, 54–71. [[CrossRef](#)] [[PubMed](#)]
15. Lehmann, J.; Joseph, S. (Eds.) *Biochar for Environmental Management: Science, Technology and Implementation*; Routledge: London, UK, 2015.
16. Lehmann, J. A handful of carbon. *Nature* **2007**, *447*, 143–144. [[CrossRef](#)] [[PubMed](#)]
17. Taghizadeh-Toosi, A.; Clough, T.J.; Condron, L.M.; Sherlock, R.R.; Anderson, C.R.; Craigie, R.A. Biochar incorporation into pasture soil suppresses in situ nitrous oxide emissions from ruminant urine patches. *J. Environ. Qual.* **2011**, *40*, 468–476. [[CrossRef](#)] [[PubMed](#)]
18. Gascó, G.; Blanco, C.G.; Guerrero, F.; Lázaro, A.M. The influence of organic matter on sewage sludge pyrolysis. *J. Anal. Pyrol.* **2005**, *74*, 413–420.
19. He, Y.D.; Zhai, Y.B.; Li, C.T.; Yang, F.; Chen, L.; Fan, X.P.; Fu, Z.M. The fate of Cu, Zn, Pb and Cd during the pyrolysis of sewage sludge at different temperatures. *Environ. Technol.* **2010**, *31*, 567–574. [[CrossRef](#)] [[PubMed](#)]
20. Hwang, I.H.; Ouchi, Y.; Matsuto, T. Characteristics of leachate from pyrolysis residue of sewage sludge. *Chemosphere* **2007**, *68*, 1913–1919. [[CrossRef](#)] [[PubMed](#)]
21. Taek-Keun, O.; Bongsu, C.; Yoshiyuki, S.; Jiro, C. Characterization of biochar derived from three types of biomass. *J. Fac. Agric. Kyushu Univ.* **2012**, *57*, 61–66.
22. Agrafioti, E.; Bouras, G.; Kalderis, D.; Diamadopoulos, E. Biochar production by sewage sludge pyrolysis. *J. Anal. Appl. Pyrol.* **2013**, *101*, 72–78. [[CrossRef](#)]
23. Thangarajan, R.; Bolan, N.; Mandal, S.; Kunhikrishnan, A.; Choppala, G.; Karunanithi, R.; Qi, F. *Biochar for Inorganic Contaminant Management in Soil. Biochar Production, Characterization, and Applications*; CRC Press, Taylor & Francis: Boca Raton, FL, USA, 2015; pp. 100–138.
24. Ok, Y.S.; Uchimiya, S.M.; Chang, S.X.; Bolan, N. *Biochar: Production, Characterization, and Applications*; CRC Press: Boca Raton, FL, USA, 2015.
25. Mukome, F.N.D.; Parikh, S.J. *Chemical, Physical, and Surface Characterization of Biochar*; CRC Press: Boca Raton, FL, USA, 2015; pp. 68–96.
26. Rodríguez, N.H.; Ramírez, S.M.; Varela, M.B.; Guillem, M.; Puig, J.; Larrotcha, E.; Flores, J. Re-use of drinking water treatment plant (DWTP) sludge: Characterization and technological behaviour of cement mortars with atomized sludge additions. *Cem. Concr. Res.* **2010**, *40*, 778–786. [[CrossRef](#)]
27. Oinuma, K.; Hayashi, H. Infrared study of mixed-layer clay minerals. *Am. Mineral.* **1965**, *50*, 1213–1227.
28. Danková, Z.; Mockovčiaková, A.; Dolinská, S. Influence of ultrasound irradiation on cadmium cations adsorption by montmorillonite. *Desalin. Water Treat.* **2014**, *52*, 5462–5469. [[CrossRef](#)]
29. Zhang, J.; Gong, J.L.; Zenga, G.M.; Ou, X.M.; Jiang, Y.; Chang, Y.N.; Liu, H.Y. Simultaneous removal of humic acid/fulvic acid and lead from landfill leachate using magnetic graphene oxide. *Appl. Surf. Sci.* **2016**, *370*, 335–350. [[CrossRef](#)]
30. Wu, P.; Zhang, Q.; Dai, Y.; Zhu, N.; Dang, Z.; Li, P.; Wang, X. Adsorption of Cu (II), Cd (II) and Cr (III) ions from aqueous solutions on humic acid modified Ca-montmorillonite. *Geoderma* **2011**, *164*, 215–219. [[CrossRef](#)]
31. Guizani, C.; Jeguirim, M.; Valin, S.; Limousy, L.; Salvador, S. Biomass chars: The effects of pyrolysis conditions on their morphology, structure, chemical properties and reactivity. *Energies* **2017**, *10*, 796. [[CrossRef](#)]
32. Tantawy, M.A. Characterization and pozzolanic properties of calcined alum sludge. *Mater. Res. Bull.* **2015**, 415–421. [[CrossRef](#)]
33. Bera, T.; Purakayastha, T.J.; Patra, A.K.; Datta, S.C. Comparative analysis of physicochemical, nutrient, and spectral properties of agricultural residue biochars as influenced by pyrolysis temperatures. *J. Mater. Cycles Waste Manag.* **2017**, 1–13. [[CrossRef](#)]

34. Huang, C.-H.; Wang, S.-Y. Application of water treatment sludge in the manufacturing of lightweight aggregate. *Construct. Build. Mater.* **2013**, *43*, 174–183. [[CrossRef](#)]
35. Wolff, E.; Schwabe, W.K.; Conceição, S.V. Utilization of water treatment plant sludge in structural ceramics. *J. Clean. Prod.* **2015**, *96*, 282–289. [[CrossRef](#)]
36. Kizinievič, O.; Žurauskienė, R.; Kizinievič, V.; Žurauskas, R. Utilisation of sludge waste from water treatment for ceramic products. *Construct. Build. Mater.* **2013**, *41*, 464–473. [[CrossRef](#)]
37. Chiang, K.Y.; Chou, P.H.; Hua, C.R.; Chien, K.L.; Cheeseman, C. Lightweight bricks manufactured from water treatment sludge and rice husks. *J. Hazard. Mater.* **2009**, *171*, 76–82. [[CrossRef](#)] [[PubMed](#)]
38. Matilainen, A.; Gjessing, E.T.; Lahtinen, T.; Hed, L.; Bhatnagar, A.; Sillanpää, M. An overview of the methods used in the characterisation of natural organic matter (NOM) in relation to drinking water treatment. *Chemosphere* **2011**, *83*, 1431–1442. [[CrossRef](#)] [[PubMed](#)]
39. Tang, W.W.; Zeng, G.M.; Gong, J.L.; Liang, J.; Xu, P.; Zhang, C.; Huang, B.B. Impact of humic/fulvic acid on the removal of heavy metals from aqueous solutions using nanomaterials: A review. *Sci. Total Environ.* **2014**, *468*, 1014–1027. [[CrossRef](#)] [[PubMed](#)]



© 2018 by the authors. Licensee MDPI, Basel, Switzerland. This article is an open access article distributed under the terms and conditions of the Creative Commons Attribution (CC BY) license (<http://creativecommons.org/licenses/by/4.0/>).